Neural Computing and Applications (2019) 31:6401–6418
https://doi.org/10.1007/s00521-018-3418-0

ORIGINAL ARTICLE

A BBO-based algorithm for slope stability analysis by locating critical failure surface

Jayraj Singh[1] · Haider Banka[1] · Amit Kumar Verma[2]

Received: 28 March 2017 / Accepted: 3 March 2018 / Published online: 4 April 2018

Abstract
Determination of the critical failure surface is performed in stability evaluation process for road cut slope, embankments, dam, excavations, retaining walls and many more. Finding the critical failure surface in a rock or soil slope is very cumbersome and becomes a difficult constrained global optimization problem. Due to existence of discontinuous function and strong multiple local minima points, researchers are facing difficulties to employ trial-and-error methods in a large search space. Thus, classical optimization techniques fail to converge to a valid solution. In this study a stochastic method called biogeography-based optimization algorithm was adopted for analyzing the factor of safety. Based on the finding from the implementation and quantitative evaluation, it was found that the proposed method for locating critical failure surface in homogeneous soil slope acquires more efficient results over other implemented methods such as grid search and genetic algorithm. The validation and effectiveness of the proposed method are investigated by solving two benchmark case studies from the literature, while the simulation design for slip surfaces is carried out using 'Rocscience slide' software tool for comparing the results.

Keywords Slope stability analysis · Critical failure surface · Factor of safety · BBO algorithm

1 Introduction

Slope stability evaluation is a classical problem in the field of civil, mining, hydraulic and geotechnical engineering. The recognition of safe design of human-made or natural slopes is achieved by assessing the stability analysis. The stability analysis includes the study of a wide range of ground movements or slope failures influenced by gravity. These failures may arise due to earthquake, floods, landslides and many other geohazards. These failures can often catastrophic and sometimes involve the extensive loss of economy, social and environment damage. In recent years, numerous methods have been developed to access the failure mechanism and to understand the instability due to geological, hydrological, seismology and geotechnical exploration. But due to existing lots of imprecision and uncertainties and many complex decision-making problems encountered in the actual scenario make the slope stability as a very challenging task. Many stochastic and fuzzy-based techniques [1–4] have been rapidly increased to solve such problems. Locating the critical slip surface associated with least factor of safety value is traditionally performed to estimate the slope stability. It is an NP-hard, unconstrained global optimization problem due to its discontinuous function and several local minima points available in the search space. In this concern, the slip surfaces with its corresponding forces such as the forces tending to make slope down, restored forces which stabilized the slope mass are essential to evaluate the available safety margin. Various approaches such as finite element method, rigid element method, limit equilibrium method, limit analysis method, distinct element method, probabilistic analysis methods and others have been used for

✉ Jayraj Singh
jayrajsingh@cse.ism.ac.in

Haider Banka
banka.h.cse@ismdhanbad.ac.in

Amit Kumar Verma
verma.ak.me@ismdhanbad.ac.in

[1] Department of Computer Science & Engineering, Indian Institute of Technology (ISM), Dhanbad, India

[2] Department of Mining Engineering, Indian Institute of Technology (ISM), Dhanbad, India

such analysis. But, the most widely analytical technique used for geotechnical analysis is limit equilibrium [5]. In limit equilibrium analysis (LEM), some methods of slice, such as Fellenius method [6], Bishop method [7], Morgenstern and Price [8], Spencer method [9], Janbu method [10] and others, derive factor of safety based on some assumption criteria [11]. The essence of these methods is to divide the whole sliding slope mass into a finite number of vertical slices and evaluate the slip surfaces to calculate the factor of safety margin in terms of different acting forces. To evaluate the slip surfaces in a large search space made the safety factor margin big and prove to be a difficult problem in the field of geotechnical engineering. Ching and Fredlund [12] discussed some encountered problems associated with the limit equilibrium methods of slices. Baker and Garber [13] also demonstrated the problem of limiting equilibrium in terms of the variational calculus, and then, it is proven that the minimal factor of safety must occur on slip surfaces with a special geometric property. Trial-and-error methods are also not found suitable due to lack of engineer's experience or high solution search space [14]. The factor of safety function is often highly multimodal, and it is certainly nonsmooth due to varying the soil parameters, ground condition and external loads. In the presence of several local minima points in the search space and high computational complexity environment, classical techniques fail to give a valid solution. In the presence of these disadvantages, stochastic techniques could efficiently approximate the optimal solution to such kind of problems. Yamagami and Ueta [15] used some stochastic approach such as BFGS and DFP method to investigate the factor of safety of the different slopes. In a similar way, an extensive number of stochastic approaches [16–19] also received a lot of attention, because of its elegance and efficiency. Many researchers have successfully employed meta-heuristic optimization algorithms for slope stability problems, such as: Greco [14] used Monte Carlo technique; Chen and Morgenstern [20], McCombie and Wilkinson [21], Das [22], Zolfaghari et al. [23], Jianping et al. [24] and Sengupta and Upadhyay [25] used different search techniques like grid method and genetic algorithm. Kahatadeniya et al. [26] used ant colony optimization. Ahangar-Asr et al. [27] applied evolutionary polynomial regression (EPR)-based approach for analyzing the slope stability of soil and rock slopes. Khajehzadeh et al. [28, 29] have implemented a new metaheuristic approach GSA based on the law of gravity and motion. And Kashani et al. [30] used ICA-based search for slope stability problems.

In the present study, the biogeography-based optimization (BBO) algorithm is employed to locate the margin of the safety factor. This algorithm has been widely adopted due to its ease of implementation and ability to solve highly complex, nonlinear optimization problems. The Fellenius method from LEM's methods of the slice is defined as an objective function to calculate the factor of safety. The effectiveness of the proposed method is investigated by solving two benchmark problems from the literature, where the simulation design for slip surface model is compared using 'Rocscience slide' software tool for validating the results. From the implementation result and quantitative evaluation, it is clearly visible that the proposed method for locating critical failure surface for homogeneous soil slope acquires more efficient results over implemented methods.

2 Slope stability analysis

The slope stability analysis is done through many conventional methods such as numerical methods, kinematics methods, probabilistic methods, limit equilibrium methods, imperial methods [27, 31]. The most widely analytical technique used for geotechnical analysis is limit equilibrium [28–34], which calculates the safety factor based on the Mohr's coulomb criteria. In this study, the procedure based on the method of slices is to run a large number of iterations to locate the critical failure surface, where the center coordinate points and radius of the circle are varied until the slip surface for which the factor of safety would be minimum. The essence of this method is to divide the whole sliding slope mass into a finite number of vertical slices so that the comparison between the total available shear strength along the slip surface with total forces acted in the slice's face required to be in equilibrium state could easily derive. In the proposed methodology, a finite number of valid slip surfaces are only computed, whereas the invalid surfaces which yield the unreasonable FoS values are ignored. The methodology for evaluating the failure surface is illustrated in Fig. 1.

2.1 Formulation of slip surface

A 2-dimensional slip surface is formulated here. The failure direction and the x–y plane where the search procedure for slip surface is to made must be specified. In this study, the prime objective is to locate the critical failure surface—a surface along which the rock mass or soil is more likely to fail. This 'likelihood-to-fail' is quantified by the factor of safety, which is associated with a unique slip surface. This slip surface is described by a polyline of 2-dimensional-N-points $\{P_0, P_1, P_2, \ldots, P_n - 2, P_n - 1\}$. It must satisfy all its kinematic and geometric constraints [24]. Here, the slip surface is considered as a function F(P).

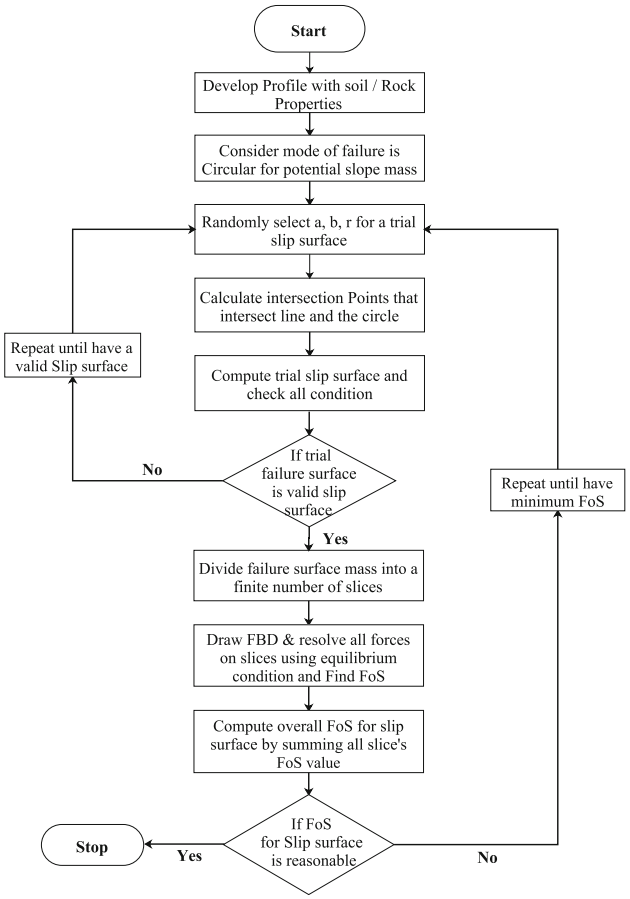

Fig. 1 Transition workflow diagram for slope stability analysis

$$\boldsymbol{P} = \begin{bmatrix} \boldsymbol{P_0} = \text{slope}(t_0) = (x_0, y_0) \\ \boldsymbol{P_1} = (x_0, y_0) \\ \cdots \\ \boldsymbol{P_i} = (x_i, y_i) \\ \cdots \\ \boldsymbol{P_{n-2}} = (x_{n-2}, y_{n-2}) \\ \boldsymbol{P_{n-1}} = \text{slope}(t_{n-1}) = (x_{n-1}, y_{n-1}) \end{bmatrix} \tag{1}$$

where positional vector matrix (P) is a solution vector and represents a polyline that describes a failure surface. The function F(P) shown in Eq. 1 consumes n-points of a polyline as inputs while outputting a scalar factor of safety value associated with a failure surface [35, 36]. However, F(P) function is often highly discontinuous as well as multimodal when its all geometric and kinematic constraints are being satisfied. Sometimes, multimodality may be the results from the multilayering of the soil or mineral lenses in the potential mass. In the research of Chen and Shao [37], it is clearly demonstrated that there may be several local minima presented in the solution space. Hence, the function F(P) is here certainly nonsmooth and being regarded as an NP-complete problem. These all pertain to make the considered problem as a global optimization problem [36, 37].

2.1.1 Dimension of the problem

The dimension of the problem will be dictated by the number of vertices which describe a slip surface from bottom to top. Each inner vertex of the slip circle contributes to two extra dimensions, while single parametric values are needed to describe the entry and exit vertex surface since both must lie on the slope surface. Thus, a failure surface of n vertices (i.e., including entry and exit points) will translate to $2 \times (n-1)$ a dimension problem [35, 38].

2.1.2 Constraints and Bounds

Let us consider, a Cartesian, X–Y plane shown in Fig. 2, the function $y = S(x)$ represents slip surface, while the bedrock surface is described by $y = R(x)$. In order to satisfy all kinematic and geometric conditions, for a potential failure surface, some geometric constraints are very necessary to bind to the surface to make in equilibrium. These constraints will define the domains for each $2n-2$ control variables [39]. The slope surface is first parameterized from right to left between 0 and 1, and as such, $t_0, t_{n-1} | t_0 > t_{n-1} \in [0,1]$ define the entry and exit point of the failure surface. This generates points $p_0 = \text{slope}\ (t_0) = (x_0, y_0)$ and point $p_{n-1} = \text{slope}\ (t_{n-1}) = (x_{n-1}, y_{n-1})$.

2.1.3 Bounds for *x*-coordinates

The failure surface of n vertices can be divided equally from x_0 and x_{n-1} to generate $n-2$ slices. These slices bound the set of x-coordinates such that-

$$\begin{aligned} &x_i > x_j \,|\, j > i \quad \forall\, x_i = 1, 2, 3, \ldots, n-2, \text{ and} \\ &\quad x_j = 2, 3, 4, \ldots n-1 \\ &\quad \text{where } x_i \in \left(x_{i-1}, x_{i-1} - \frac{x_{n-1} - x_0}{n-2} \right) \end{aligned} \tag{2}$$

Since, the distance between each vertices $(P_0, P_1, \ldots P_{n-1})$ are equal. That is,

$$\begin{aligned} &(x_i - x_{i+1}) = (x_{i+1} - x_{i+2}) = \cdots = \left(\frac{x_{n-1} - x_0}{n-2} \right), \\ &\quad \text{where } i \in [0, n-1] \end{aligned} \tag{3}$$

2.1.4 Bounds for *y*-coordinates

The control variables y_0 and y_{n-1} directly depend on slope height and base of the slope which can be determined easily from the slope geometry, while remaining $2n-2$

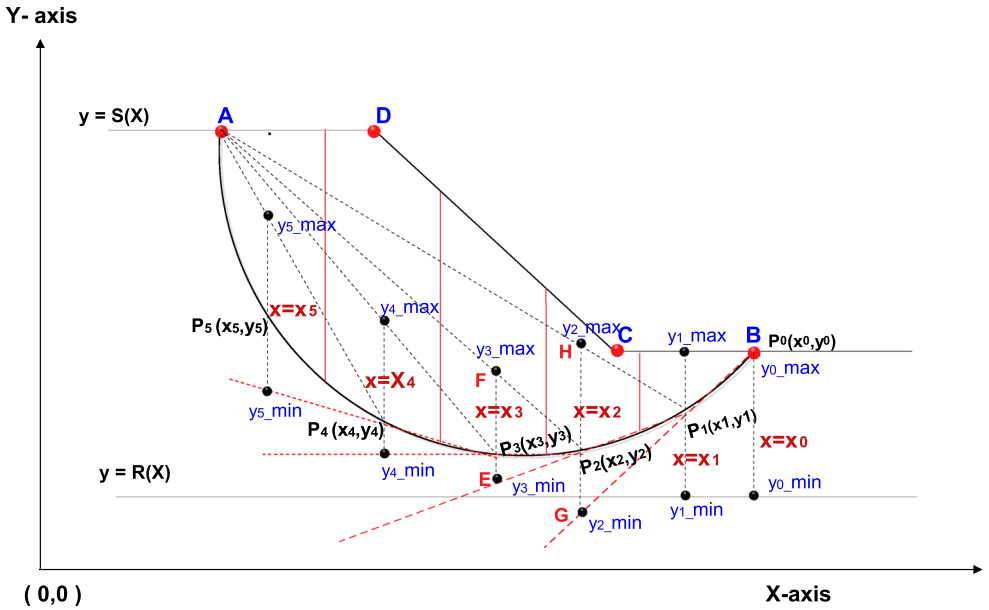

Fig. 2 Control variables for an admissible slip surface

variables i.e., $\{x_0, (x_1, y_1), \ldots, (x_i, y_i), \ldots, (x_{n-2}, y_{n-2}), (x_{n-1})\}$ will be derived as per the coordinate system for slip surface. Cheng [36] proposed in his study that if the value of x_1 to x_{n-1} are defined, then corresponding lower bounds and upper bounds to $(y_2, \ldots, y_n)$ are then calculated by utilizing the geometry and bed rock [40, 41]. The bounds on the control variable should be dynamic for being an admissible surface. The bounds for y_0-coordinate will be-

$$y_0 \in \big((R_x), (S_x)\big) \tag{4}$$

As the line connecting points p_{n-1} and p_1, intersects with the line $x = x_2$ at point H with y-coordinate y_H and a line passing through p_0 and p_1 which is extended to interact with the line $x = x_2$ at point G with y-coordinate y_G determine. Hence $\{y_{2min}, y_{2max}\}$ can be determined as $y_{2_{\min}} = \max(y_G, R(x_3))$ and $y_{2_{\max}} = \min(y_H, y_0(x_3))$. Similarly, the bounds on y-coordinate of each point on the slip surface, i.e., $\{y_{1\min}, y_{1\max}, \ldots, y_{n-1_{\min}}, y_{n-1_{\max}}\}$ shown in Fig. 2, can be determined by the relation,

$$y_i \in \left(\big(\mathrm{Max}(R_{(x_i)}), Y_{i_{\min}}\big), \big(\mathrm{Min}(S_{(x_i)}), Y_{i_{\max}}\big) \right) \tag{5}$$

$$\text{where} \quad Y_{i_{\min}} = y_{i-1} + \left(\frac{y_{i-1} - y_{i-2}}{x_{i-1} - x_{i-2}} \right)(x_i - x_{i-1}) \tag{6}$$

$$Y_{i_{\max}} = y_{i-1} + \left(\frac{y_{n-1} - y_{i-1}}{x_{n-1} - x_{i-1}} \right)(x_i - x_{i-1}) \tag{7}$$

2.2 Modeling the objective function

In this study, the development of the objective function is made for employing the BBO algorithm. The factor of safety equation derived using Fellenius method [6, 32] is defined as the objective function or fitness function for the algorithm. In Fellenious method, the slope failure is considered to be in circular shape, while the slide side forces E_1, E_2 and X_1, X_2 shown in Fig. 3 are assumed to be negligible. In this study, the objective function is chosen here to be express a safety factor of a circular slip surface, where it would be derived in terms of center points (a, b) and radius (R). In regard to proceed this, a circular surface is drawn within its slope geometry by random selection of a center point (a, b) and radius (R). The intersection points that meet the circular surface and slope boundary are derived. The circular arc path (AB is shown in Fig. 3) is assumed to be a failure surface with center 'O' and radius 'R.' The whole slope mass (ABCD) is divided into a finite number of slices which are depicted in Fig. 3 so that the total available shear strength (resisting force F_r) and total shear stress (deriving force F_d) can be easily calculated. The Fellenius factor of safety equation is expressed as

$$F = \sum_{i=1}^{n} \frac{F_r}{F_d} = \frac{\sum_{i=1}^{n} [c_i' l_i + (W_i \cos\alpha_i - \mu_i l_i) \tan(\phi_i')]}{\sum_{i=1}^{n} W_i \sin\alpha_i} \tag{8}$$

Finally, the working of BBO algorithm is mentioned for minimization of the objective function. The center coordinates and radius are varied in every iteration until the slip surface whose corresponding factor of safety (FoS) is found minimum.

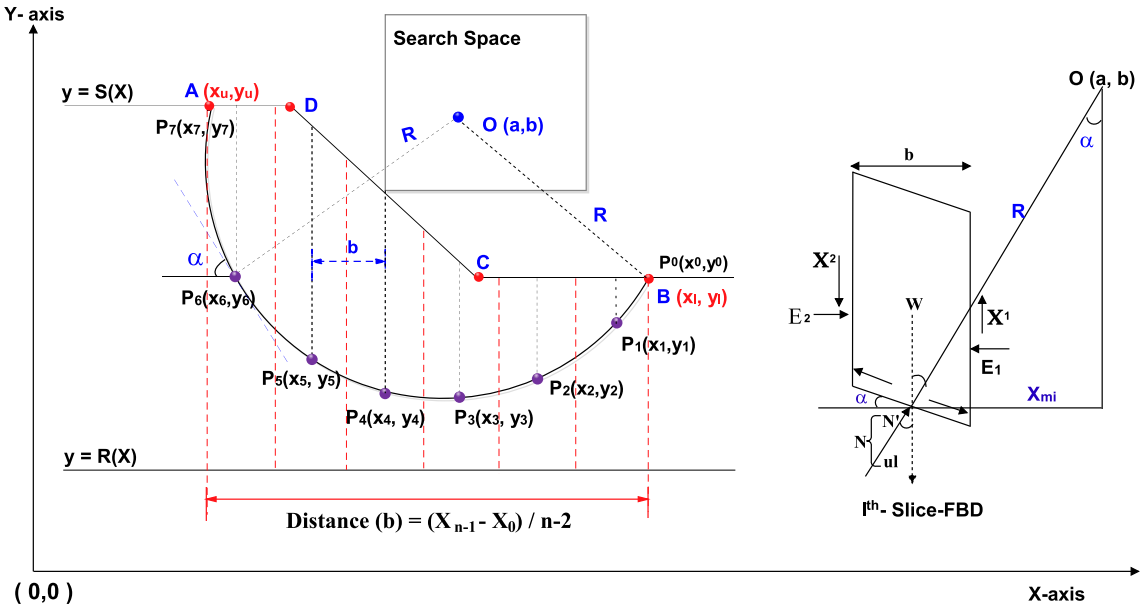

Fig. 3 Slip surface of having finite vertical slices with FBD

2.2.1 Derivation of failure slip surface in terms of (a, b, R)

To employ the BBO algorithm, the factor of safety (FoS) is defined as the fitness function, which must be derived in terms of the center point (a, b) and radius (R) of the circular surface. In the next stage, the development of objective function is built. First, we determine the intersection points that meet the circular path with the sloped boundary and then the distance from top to bottom of the circular failure surface is calculated for finding the width of the slices. Finally, the point of intersection with the middle of the slice and boundary of slip surface is calculated for deriving the base angle (α) of the slice. Let $(x_1, y_1)(x_2, y_2), \ldots, (x_n, y_n)$ are the coordinates of intersection points of the failure slip surface with the middle of n-slice in the direction from foot to top of the slope, where the height of the slope is $y = h$.

The equation of circle is:

$$(x-a)^2 + (y-b)^2 = R^2 \tag{9}$$

The intersection points (x_l, y_l) and (x_U, y_U) of a circle and a line of the form $y = mx + d$ are as follows:

$$x_{l,u} = \frac{a + bm - dm \pm \sqrt{\partial}}{1 + m^2} \tag{10}$$

where $\partial = r^2(1 + m^2) - (b - ma - d)^2$

$$y_{l,u} = \sqrt{(R^2 - (x_{l,u} - a)^2)} + b \tag{11}$$

If the intersection points are not in slope region, it will be corrected using geometry so that an admissible failure surface is created with valid intersection points on slip surface. Now, the width of slices can be determined as

$$\text{Width of each slice (b)} = \frac{|x_u - x_l|}{n} \tag{12}$$

where n = number of slices divided in the region. Now, using geometry the angle of slice base (α) with the tangent at intersection point (x_{mi}, y_{mi}) is derived. A free body diagram (FBD) of ith- slice and angle of slice base is shown in right of Fig. 3.

$$\text{Angle of slice base}(\alpha) = \sin^{-1}\left(\frac{x_{mi}}{R}\right) \tag{13}$$

where $x_{mi} = x_i - b/2$ and $y_{mi} = \sqrt{(R^2 - (x_{mi} - a)^2)} + b$

Now, other terms that come into play in the derivation for factor of safety (FoS) will be calculated as follows:

$$\text{Length of Slice}(L) = \frac{b}{\cos\alpha} \tag{14}$$

$$\text{Tengential force at each slice } (T) = w * \sin(\alpha) = \gamma * h * b * \sin(\alpha) \tag{15}$$

$$\text{Normal force at each slice } (N) = w * \cos(\alpha) = \gamma * h * b * \cos(\alpha) \tag{16}$$

Thus, all the terms are calculated here. Now, by substituting all these terms associated with each slice in Eq. 8, the factor of safety (FoS) value corresponding to a failure surface is derived. Algorithm 1 illustrates the pseudocode for deriving factor of safety for slope surface.

Algorithm 1: Pseudocode for deriving factor of safety (FoS) of slip surface.

Inputs:

1. Constant parameters: *Cohesion (C), Pore-pressure (μ), Friction angle (ϕ), UnitWeight (λ).*
2. Varying parameters: *Centre points (a, b), radius(R)*

Result: Factor of safety (FoS) for a failure surface

Step 1: Initialize slope surface geometry.
Step 2: /* Derive the slip surface in terms of (a,b) and R */ .
while *Slip surface!= valid surface* **do**
  2.1 Randomly select 'a, b, R' for a slip surface
  2.2 Find intersection points (x_L, y_L) and (x_U, y_U) between slope boundary surface and slip circle
  2.3 Divide the slope mass into n-finite slices
  2.3 Derive all n-points $\{P_1(x_1, y_1), P_2(x_2, y_2), ..., P_n(x_n, y_n)\}$ that define in n-2 slices of failure slip surface.
end
Step 3:
for $i = 0$ *to* $n-2$ /* $n-2$ = *number of slices*/ **do**
  3.1 Derive width(b), Angle of Slice base (α), Tengential force on slice, Normal force on the slice
  3.2 Calculate $(FoS)_i$ for i^{th}-slice /* Use Eq. 1 */
end
Step 4:
4.1 Calculate Factor of safety $(FoS)_{failure\ surface} = \frac{1}{n}\sum_{i=1}^{n}(FoS)_i$
Step 5: Stop

3 Working principle of biogeography-based optimization algorithm

Biogeography-based optimization (BBO) is a stochastic random search algorithm inspired from island biogeography [42]. It presents the robustness of the optimum solution to many complex-type engineering problems. BBO algorithm has been widely adopted due to its ease of implementation and the ability to solve highly nonlinear problems. With these advantages, BBO algorithm has been used in many applications recently, such as classification [43, 44], sequence alignment [45], TSP problems [46] and other global optimization problems. The algorithm examines the factors that affect the distribution of biological species among neighboring islands [47, 48]. The algorithm is implemented typically with a population of possible solutions and uses probabilistic transition rules instead of deterministic rules, whereas the classical optimization techniques such as linear programming and integer programming work with a single solution [49]. The algorithm starts with the initialization of the population (called habitats). Each habitat represents a possible solution of the problem under consideration. Every solution or habitat is a collection of suitability index variables (SIVs), where SIVs indicate the independent variables of the habitat (features of the solution) that represents suitability of the habitat to which it belongs. Similarly, another habitat suitability index (HSI) relates the dependent variables associated with goodness of habitat solution. The BBO approach describes the immigration and emigration of species between habitats. High HSI of the habitat is analogous to good solutions and will be occupied by a large number of species, so it is having a high emigration rate and low immigration rate (since the habitat is nearly saturated with species), while low HSI habitat is analogous to poor solution and will be having a small number of species. Through the migration operation, high HSI solutions share a lot of features with poor solutions and poor solutions can accept a lot of features from good solutions [47]. This probabilistic operation (migration) modifies SIVs of the habitats based on the immigration rate (λ_i) and the emigration rate (μ_i), where both λ_i and μ_i are the functions of a number of species in ith habitat (H_i). For mathematical convenience, it is assumed that the immigration rate (λ_i) and emigration rate (μ_i) are linear functions of the number of species. The linear migration model for ith habitat is formulated using Eqs. 17 and 18.

$$\lambda_i = I * (1 - n_i)/n \tag{17}$$

$$\mu_i = E * n_i/n \tag{18}$$

where I and E represent the maximum possible immigration and emigration rate, 'n' indicates the maximum number of species, and n_i is the number of species in the ith habitat.

The relationship between species count (S), maximum immigration (I) and emigration rate (E) is illustrated in Fig. 4, where 'S_0' is the equilibrium number of species and $S_{\max}$ is the maximum species count. The decision to modify each solution is taken based on the immigration rate of the solution. After following migration operation habitats go through the mutation process for maintaining the diversity among the population. In this process of mutation, a change is made by replacing an HSI from the habitat with another randomly generated HSI with a very low probability [47]. Each candidate solution is associated with a mutation probability defined by Eq. 19.

$$M(s) = \frac{M_{\max}(1 - Ps)}{P_{\max}} \tag{19}$$

Here, $M_{\max}$ is a user-defined parameter, Ps is the species count of the habitat, $P_{\max}$ is the maximum species count. Finally, the whole process is run for a consecutive number of generations until to have a minimum objective function value is attained. Figure 5 represents the workflow diagram for the whole BBO process.

4 Implementation of BBO algorithm in failure slip surface analysis

To implement the BBO algorithm, the factor of safety (FoS) function is defined as fitness function which is derived in terms of the center coordinates (a, b) and radius (R) of the circular surface. The Fellenius method [6] from limit equilibrium methods is used to derive the factor of safety (FoS). The analysis of the problem can be considered in two stages. In the first stage, development of objective function is built, which is demonstrated in Sect. 2.2, while in a second stage the working of BBO is mentioned for minimization of the fitness function using migration and mutation operation. Further, the population passes through elitism mechanism, where a habitat with

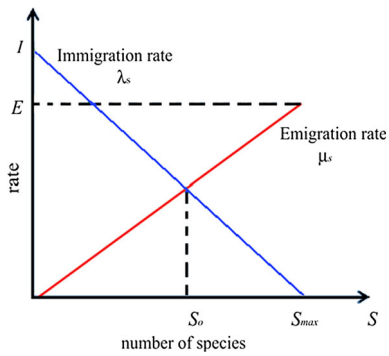

Fig. 4 Species model for species count, immigration rate and emigration rate relationship

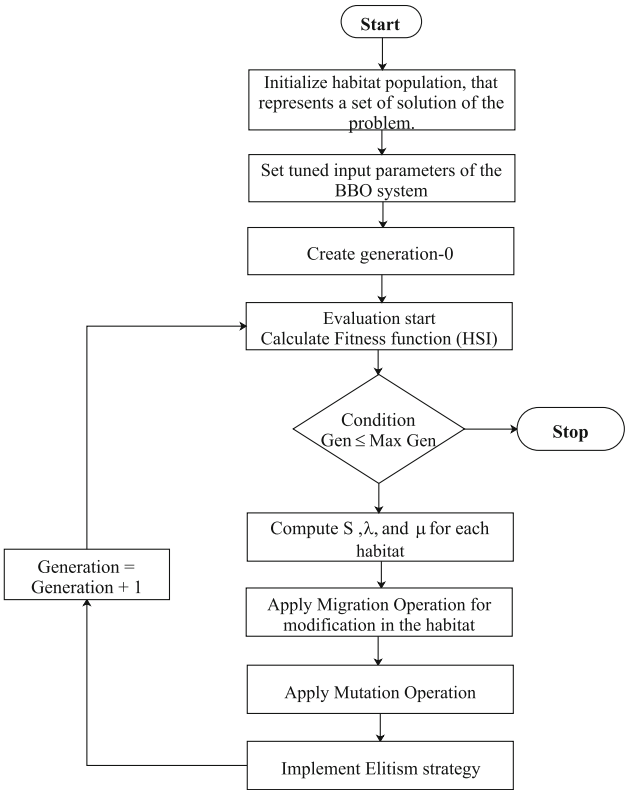

Fig. 5 Flowchart of BBO algorithm

best fitness value is chosen to pass in the next generation for preserving the solution quality. Real values are coded for the variables in the derivation of the fitness function, while the parameters of the algorithms such as population size, emigration rate (E), immigration rate (I), mutation rate ($M_{\max}$) are fine-tuned with the best values in the implementation. The proposed BBO algorithm has the following steps:

4.1 Generating population

In the first step of implementation, a number of habitat population are generated, where each population constitutes with no. of variables and represents a solution in search space. The variables (a, b, R) in the population are chosen randomly within its range, and then intersection points (x_l, y_l), (x_u, y_u) of circular surface are derived. Thus, a typical habitat design with 7 variables like $a|b|R|x_l|y_l|x_u|y_u$ computes a slip surface. During the implementation process, the real values are used for each variable, while the range of variables is tuned according to the problem under consideration. The encoding representation of a slip surface from a habitat is shown in Fig. 6.

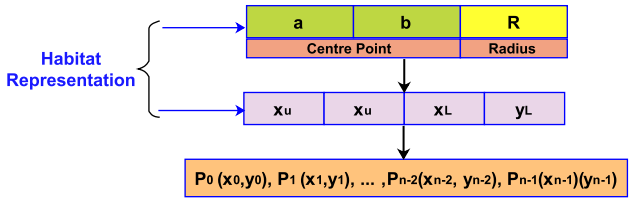

Fig. 6 Pictorial view of a habitat structure to represent a failure slip surface

4.2 Migration and mutation

The migration operation in BBO is used to diversify the solution space. It generally explores the whole solution search space. In this process, a pair of habitat is picked up on the basis of migration rate and emigration rate and then exchanges the variables (features) of high HSI habitat to low HSI to improve the solution quality [50]. The probability of the habitat (H_i) to be modified is proportional to its immigration rate (λ_i), while the probability of exchange variables from the source habitat (H_j) is proportional to the emigration rate (μ_j). This migration between variables of habitats can be expressed using Eq. 20.

$$H_i(SIV) = H_j(SIV) \tag{20}$$

The pseudocode for the whole migration process is depicted in Algorithm 2. After cross-exchange of variables (migration) between habitats, the FoS values for all possible habitats are calculated. The habitat having lower fitness value is chosen for participating in next further process, while habitats associated with invalid solutions (belong to invalid surfaces) are ignored. This process can result a better habitat which is being added to the population. With this new value of habitat, the algorithm may able to produce a better solution.

Algorithm 2: Pseudocode for migration operator in BBO

```
Initialization of Population(in the form of N-habitats) ;
for i=1 to N do
    Select a SIV_i in H_i with probability ∝ λ_i ;
    (Example - H_4 is selected since its λ_4 is largest value ;
    If an SIVj is selected to be modified ;
    if (rndreal) < λ_i then
        for i=1 to N do
            Select a SIV_k in H_k with probability ∝ μ_k ;
            (Example - H5 is selected since its μ_5 is largest value (Source of
            Modification);
            if (rndreal) < μ_i then
                Randomly select SIV_j from H_i ;
                Replace a random SIV_j in H_i with an SIV_j from H_k ;
            end
        end
    end
end
```

This whole migration process is followed by mutation operation. The mutation operator generally intensifies the solution search space by altering one or more features in a habitat and gives a new solution chance to improve better fitness value. In this process, a probability is assigned to each habitat. High probability means the solution is very near to an optimum solution. If it is low, the solution is far away from the optimum solution and shows a high chance for mutation operation. Algorithm 3 shows the pseudocode for mutation process.

Algorithm 3: Pseudocode for mutation operator in BBO

```
for i=1 to N (Where N is the number of habitats) do
    for j=1 to N do
        if (H_mutate) > Rnd_real (Hmutate is a user defined parameter) then
            Randomly generate SIV_j ;
            Replace a random SIV_j in H_i with generated SIV_j.
        end
    end
end
```

5 Validation using different numerical benchmark studies

In this section, effectiveness and validation of the proposed approach are examined by solving two different numerical benchmark problems from the literature. These problems are considered for homogeneous soil slope, where the Fellenius method is considered to be used as fitness function of the algorithm. At first, the safety factor is examined using grid search (GS) method, where the center point of a failure surface falls into a specified rectangular area, whose position is determined on the basis of solid engineering experiences. In this rectangular grid, each point represents a center of slip surface on a certain radius range. Finally, on each grid point, the factor of safety is calculated to examine the minimum safety factor [51, 52]. In the similar way to validate the methodology, genetic algorithm (GA) is also implemented. In this approach, a binary-coded chromosome in the population is encoded using 24 bits (00111000|10010010|01000010) associated with its variables (a, b) and R. Each chromosome in the population described a possible solution in the search space. Finally, the minimization of the fitness function is achieved by evaluating the chromosome selected over consecutive generations where the performance has been improved by using the application of crossover, mutation operators. The remaining of the implementation have been employed the same as in the literature of Sengupta and Upadhyay [25]. In the next stage, the BBO algorithm is adopted to locate the critical failure surface associate with optimal factor of safety. The findings of this algorithm indicate that the BBO algorithm produces the minimum result more efficient with fast convergence rate. The statistical analysis of the experimental results also confirms the higher stability analysis of the algorithm.

5.1 Case study 1

The geometry of this homogeneous soil slope shown in Fig. 7 is taken from the study of Yamagami and Ueta [15].

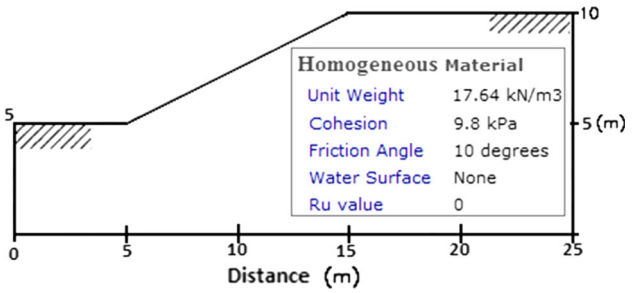

Fig. 7 Geometry and properties of slope model for case study 1

The geotechnical properties of the soil material are taken as effective internal base friction (ϕ) is 10°, effective cohesion (c) is 9.8 KPa, pore pressure (μ) is 0, unit weight (γ) is set 17.64 kN/m^3. In the proposed analysis, the above algorithms (grid search, GA and BBO) are rigorously run a consecutive number of iterations. As can be seen from Fig. 8, it has been observed after successive iterations that the factor of safety obtained by grid search and the GA is stabilized at 1.265 and 1.237, which shows the local minima. BBO algorithm has little better performance as it produces the minimum factor of safety at 1.224, which represents global minima in the search space. The tuning parameters of the algorithm which are rigorously found as best parameters to fine-tune the result are depicted in Table 1.

The critical slip surfaces located by the above algorithms over different iterations are shown in Fig. 9, whereas its associated factors of safety are tabulated in Tables 2, 3 and 4. The Tables 5, 6 and 7 illustrate the result with all slice data values for global minimum factor of safety using the above approaches (GS, GA and BBO). - From the comparative result of present method's and former studies summerized in Table 8, it is observed that the critical slip surface associated with a minimum factor of safety obtained by grid search, GA and BBO methods tends to near with previously computed values.

Table 1 Tuned BBO parameters for case study 1

Number of habitats	100
Emigration rate (E)	1
Immigration rate (I)	0.5
$M_{\max}$	0.2
Number of generation	250

5.2 Case study 2

This example problem is abstracted from the literature by Fredlund and Krahn [31]. The analysis is done for homogeneous cohesive soil slope, whereas the geotechnical properties of the material are taken as; unit weight (γ) is 120 pcf, friction angle is 20°, and effective cohesion is set at 29 KPa. The geometric view of the slope model is depicted in Fig. 10.

This problem is also examined over grid search, GA and BBO algorithm with a similar setup and objective function. The minimum safety factor has been analyzed over successive iterations. The variation of factor of safety derived by present algorithms on various consecutive generations are depicted in Fig. 12, whereas the critical failure surface associated with minimum FoS over different iterations are illustrated in Tables 9, 10 and 11. The parameters which involved in deriving the optimal factor of safety corresponding to critical failure surfaces are tabulated in Tables 12, 13 and 14.

From the result shown in Fig. 11, it is clearly understood that the grid search and GA approach would have assumed

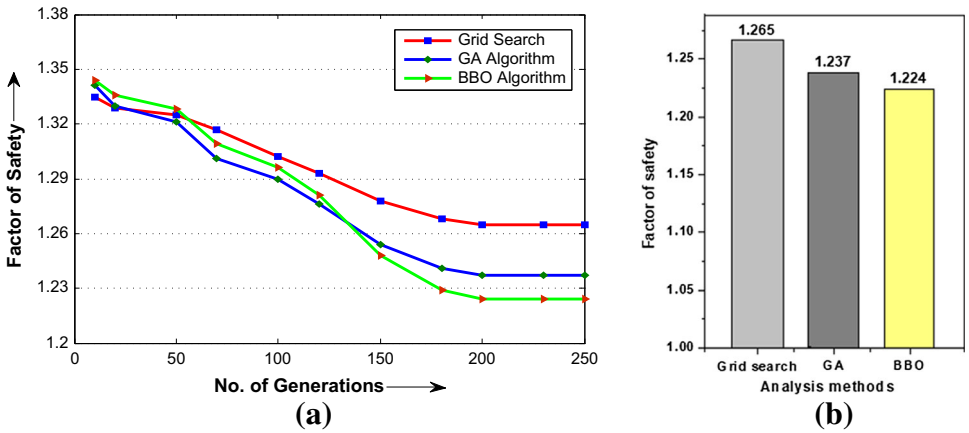

Fig. 8 The variation of FoS with no. of generation on presented methods. **a** Factor of safety versus generation graph and **b** factor of safety versus different methods

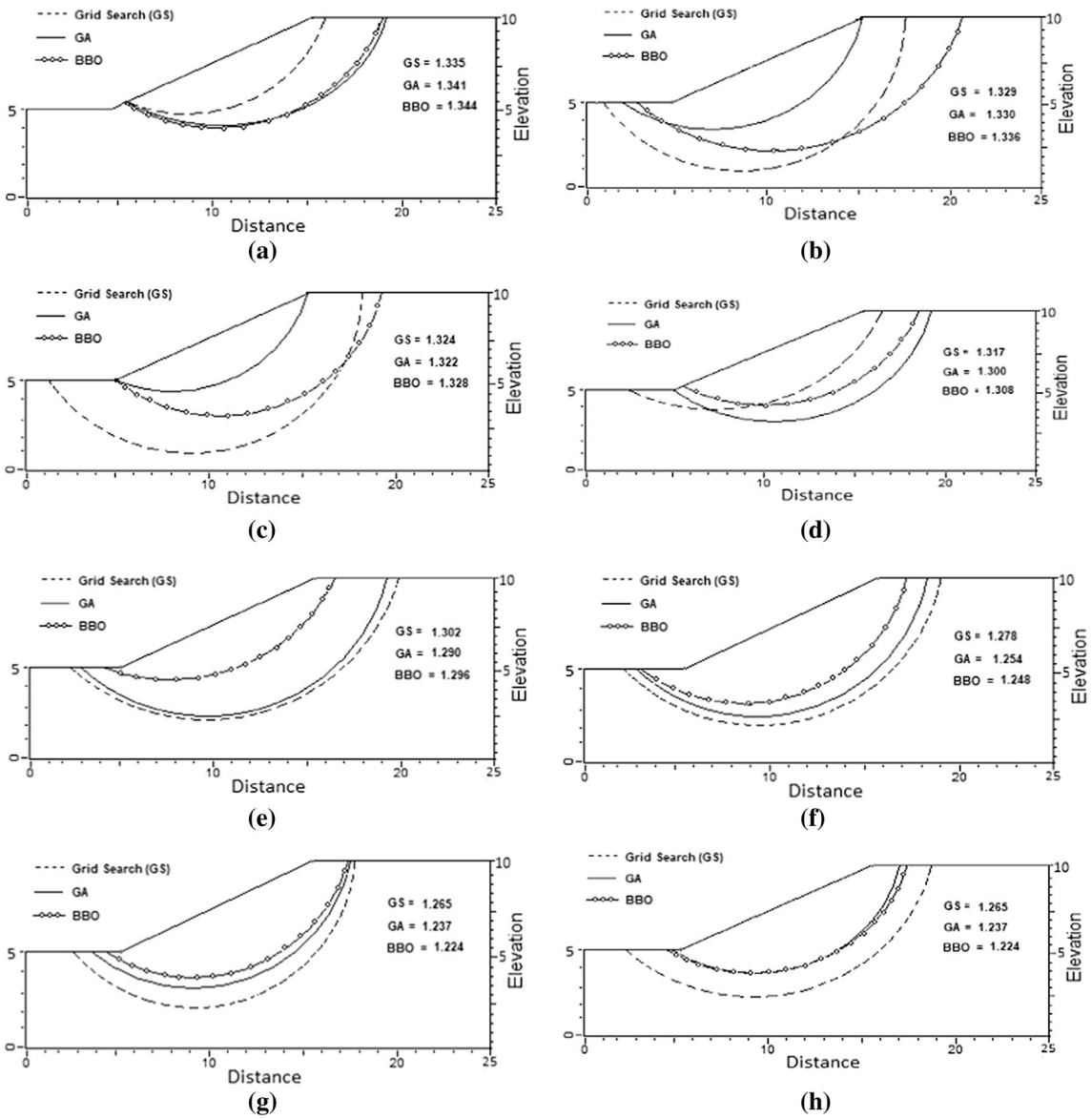

Fig. 9 Critical slip surfaces determined with Fellenious method over different generations. **a** Minimum FoS at generation 10, **b** minimum FoS at generation 20, **c** minimum FoS at generation 50, **d** minimum FoS at generation 70, **e** minimum FoS at generation 100, **f** minimum FoS at generation 150, **g** minimum FoS at generation 200 and **h** minimum FoS at generation 250

Table 2 Results for minimum FoS achieved by grid search over the iterations

No. of generation	Center point (a, b)	Radius (R)	Intersection points $(x_u, y_u), (x_l, y_l)$	Deriving moments (F_d)	Resisting moments (F_r)	FoS
10	8.98, 12.28	7.63	(16.26, 10.00) (5.75, 5.37)	142.542	190.285	1.335
20	8.76, 9.86	8.96	(17.72, 9.73) (1.24, 5.00)	317.154	421.642	1.329
50	9.12, 10.08	9.24	(18.35, 10.00) (1.41, 5.00)	332.541	440.217	1.324
70	10.56, 11.83	8.88	(19.25, 10.00) (4.90, 5.00)	330.218	250.746	1.317
100	9.69, 12.77	10.76	(20.09, 10.00) (2.25, 5.00)	324.788	422.967	1.302
150	9.07, 11.78	10.02	(18.93, 10.00) (1.70, 5.00)	320.585	409.554	1.278
200	9.12, 10.63	8.76	(17.86, 10.00) (2.40, 5.00)	290.850	367.966	1.265
250	8.98, 12.00	9.94	(18.72, 10.00) (1.93, 5.00)	306.153	387.215	1.265

Table 3 Results for minimum FoS achieved by GA over different iterations

No. of generation	Center point (a, b)	Radius (R)	Intersection points $(x_u, y_u), (x_l, y_l)$	Deriving moments (F_d)	Resisting moments (F_r)	FoS
10	10.49,13.16	9.31	(19.25,10.00) (5.54,5.27)	214.378	287.586	1.341
20	7.25,11.67	8.37	(15.46,10.00) (2.20,5.00)	188.425	250.649	1.330
50	8.10,11.95	7.59	(15.43,10.00) (5.02,5.01)	141.199	186.734	1.322
70	7.28,13.65	9.99	(16.58,10.00) (2.30,5.00)	198.630	258.228	1.30
100	9.69,12.11	9.94	(19.40,10.00),(275,5.00)	303.370	391.238	1.290
150	8.98,11.62	9.35	(18.19,10.00) (2.38,5.00)	286.851	359.657	1.254
200	8.98,11.73	8.80	(17.61,10.00) (3.31,5.00)	248.276	307.001	1.237
250	9.12,11.56	8.06	(17.02,10.00) (4.45,5.00)	208.901	258.318	1.237

Table 4 Results for minimum FoS achieved by BBO over different iterations

No. of generation	Center point (a, b)	Radius (R)	Intersection points $(x_u, y_u), (x_l, y_l)$	Deriving moments (F_d)	Resisting moments (F_r)	FoS
10	10.49,13.21	9.31	(19.23,10.00) (5.59,5.29)	211.563	284.501	1.344
20	10.44,12.88	10.80	(20.86,10.00) (3.06,5.00)	322.219	430.645	1.336
50	10.71,11.84	8.92	(19.44,10.00) (4.99,5.00)	252.598	335.565	1.328
70	10.00,13.10	9.16	(18.62,10.00) (5.39,5.19)	206.098	269.589	1.308
100	7.70,14.09	9.86	(16.67,10.00) (3.88,5.00)	172.91	224.125	1.296
150	8.27,12.83	9.51	(17.35,10.00) (2.88,5.00)	230.372	287.390	1.248
200	9.01,12.34	8.80	(17.49,10.00) (4.16,5.00)	220.695	270.105	1.224
250	9.02,12.27	8.76	(17.48,10.00) (4.15,5.00)	221.357	270.995	1.224

Table 5 Global minima safety factor computation using grid search

Slice no.	c (KPa)	μ (KPa)	ϕ (°)	b (m)	l (m)	h (m)	w (m)	α (°)	Resisting moment (F_r) $cl + (w\cos\alpha - \mu l)\tan\phi$	Deriving moment (F_d) $w\sin\alpha$
1	9.8	0	10	1.766	2.211	0.769	23.943	−37.022	25.036	−14.41
2	9.8	0	10	1.766	1.917	2.609	81.265	−22.904	31.976	−31.612
3	9.8	0	10	1.766	1.794	4.016	125.067	−10.149	39.274	−22.027
4	9.8	0	10	1.766	1.767	5.022	156.425	2.107	44.863	5.749
5	9.8	0	10	1.766	1.823	5.648	175.916	14.462	47.89	43.913
6	9.8	0	10	1.766	1.991	5.853	182.301	27.562	48.001	84.313
7	9.8	0	10	1.766	2.394	5.262	163.88	42.504	44.762	110.679
8	9.8	0	10	1.766	3.843	2.955	92.042	62.684	45.117	81.755
Factor of safety (FoS) $= \sum_{i=1}^{n} \frac{F_r}{F_d}$									FoS = 1.265	

1.928 and 1.921 to be the lowest factor of safety. But in BBO algorithm, upon increasing the number of generations and fine-tune the parameters of the algorithm, the final factor of safety stabilizes at 1.916, which represents the global minima. The tuning parameters which are rigorously found to be best for fine-tune the result are depicted in Table 15.

The comparison of results and effectiveness in terms of a minimum safety factor of the proposed method with the previous methods is summarized in Table 16.

6 Result discussion and comparison

As can be seen from the above results of the case studies, the factor of safety obtained by BBO algorithm is stabilized at lowest value as compared with grid search and GA. From the quantitative evaluation and implementation result, it is clearly visible that the BBO outperforms over these methods with stable convergence and local minima avoidance. From Fig. 8 of case study 1, it has been illustrated that grid search and GA achieved 1.265 and 1.237

Table 6 Global minima safety factor computation using genetic algorithm

Slice no.	c (KPa)	μ (KPa)	ϕ (°)	b (m)	l (m)	h (m)	w (m)	α (°)	Resisting moment (F_r) $cl + (w\cos\alpha - \mu l)\tan\phi$	Deriving moment (F_d) $w\sin\alpha$
1	9.8	0	10	1.815	2.143	0.651	20.832	−32.104	24.109	−11.066
2	9.8	0	10	1.816	1.923	2.024	64.812	−19.302	29.63	−21.413
3	9.8	0	10	1.817	1.831	3.363	107.693	−7.447	36.761	−13.952
4	9.8	0	10	1.818	1.82	4.324	138.463	4.09	42.176	9.87
5	9.8	0	10	1.819	1.887	4.913	157.343	15.798	45.171	42.815
6	9.8	0	10	1.820	2.06	5.087	162.913	28.24	45.488	77.048
7	9.8	0	10	1.821	2.457	4.672	149.598	42.38	43.557	100.795
8	9.8	0	10	1.822	3.744	2.375	76.046	61.029	43.191	66.51
Factor of safety (FoS) $= \sum_{i=1}^{n} \frac{F_r}{F_d}$									FoS = 1.237	

Table 7 Global minima safety factor computation using BBO algorithm

Slice no.	c (KPa)	μ (KPa)	ϕ (°)	b (m)	l (m)	h (m)	w (m)	α (°)	Resisting moment (F_r) $cl + (w\cos\alpha - \mu l)\tan\phi$	Deriving moment (F_d) $w\sin\alpha$
1	10	0	10	1.67	1.881	0.493	14.512	11.991	20.703	−6.672
2	10	0	10	1.67	1.735	1.972	58.099	3.409	26.858	−15.678
3	10	0	10	1.67	1.676	3.105	91.486	−5.097	32.492	−7.312
4	10	0	10	1.67	1.68	3.915	115.346	−13.718	36.673	12.688
5	10	0	10	1.67	1.751	4.399	129.594	−22.670	38.945	38.869
6	10	0	10	1.67	1.916	4.511	132.912	−32.256	39.196	65.108
7	10	0	10	1.67	2.277	4.129	121.661	−42.998	38.043	82.703
8	10	0	10	1.67	3.384	2.024	59.622	−56.118	38.349	51.854
Factor of safety (FoS) $= \sum_{i=1}^{n} \frac{F_r}{F_d}$									FoS = 1.224	

Table 8 Comparative summary of factor of safety's results for case study 1

Optimization algorithms	LEMs method	Minimum FoS
Yamagami and Ueta [15] (BFGS)	Spencer	1.338
Yamagami and Ueta [15] (DFP)	Spencer	1.338
Greco et al. [14] (Monte Carlo, pattern search)	Fellenius	1.326–1.333
Malkawi et al. [40] (Monte Carlo)	Fellenius	1.238
Solati and Habibgahi [53] (GA)	Janbu	1.380
Jianping et al. [24] (GA)	Line, spline	1.324–1.327
Kahatadeniya et al. [26] (ACO)	Morgenstern price	1.311
Kashani et al. [30] (ICA)	Spencer	1.3206
Grid search method (current study)	Fellenius	1.265
GA (current study)	Fellenius	1.237
BBO method (current study)	Fellenius	1.224

factor of safety values. But in BBO, upon increasing the number of generations and suitable tuning parameters, the factor of safety stabilizes finally at 1.224 on 250 generations. In a similar way, from Fig. 11 of case study 2, it appears that the minimum FoS value is stabilized at 1.928 and 1.921 with grid search and GA, whereas the BBO acquired at 1.916 as global optima on 200 generations. The variation of the factor of safety with the number of generations and its corresponding comparison graphs as determined by grid search, GA and BBO methods is demonstrated in Figs. 8, 9, 11 and 12. In order to obtain the reliability of the solution and validation of the proposed approach, the above results of the case studies have been validated through a Rock-science slide software tool [55].

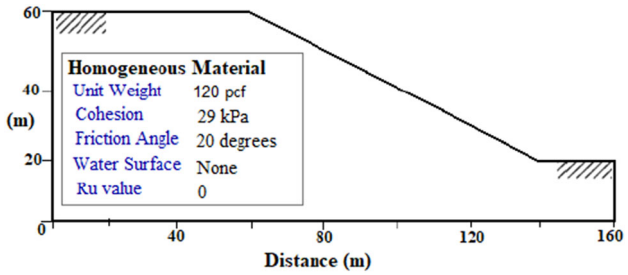

Fig. 10 Geometry and properties of slope model in case study 2

This geotechnical analysis tool includes the probabilistic analysis capabilities that statistically compute the factor of safety based on Monte Carlo or Latin hypercube simulation techniques [1, 14, 51]. In the present study, each slip surface associated with its FoS value obtained by stochastic approaches (GS, GA and BBO) over the different generations is validated over slide tool. An error between these methods is calculated to show their superiority. The maximum percentage errors between stochastic approaches with the calculated values from slide are summarized in

Table 9 Results for minimum FoS achieved by grid search over the iterations

No. of generation	Center point (a, b)	Radius (R)	Intersection points $(x_u, y_u), (x_l, y_l)$	Deriving moments (F_d)	Resisting moments (F_r)	FoS
10	105.34, 95.59	86.42	(26.59, 60.00) (147.24, 20.00)	5043.132	9760.455	1.935
20	102.22, 79.02	70.00	(34.86, 60.00) (139.91, 20.04)	4561.108	8822.250	1.934
50	102.39, 77.06	70.00	(34.51, 60.00) (142.93, 20.00)	4823.828	9326.720	1.933
70	102.39, 79.51	70.00	(35.17, 60.00) (139.58, 20.20)	4494.300	8686.462	1.933
100	103.79, 83.68	70.35	(37.54, 60.00) (136.84, 21.57)	3968.377	7660.432	1.930
120	108.84, 80.25	78.11	(33.39, 60.00) (158.56, 20.00)	5678.977	10,955.115	1.929
150	102.051, 72.65	62.76	(40.57, 60.00) (137.82, 21.08)	4180.687	8061.115	1.928
200	(144.57, 110.46)	87.18	(82.94, 48.80) (133.930, 23.93)	1448.540	2793.176	1.928

Table 10 Results for minimum FoS achieved by GA over different iterations

No. of generation	Center point (a, b)	Radius (R)	Intersection points $(x_u, y_u), (x_l, y_l)$	Deriving moments (F_d)	Resisting moments (F_r)	FoS
10	104.27, 81.76	76.79	(30.63, 60.00) (149.92, 20.00)	5348.586	10,355.853	1.936
20	109.01, 92.49	86.23	(29.13, 60.00) (155.70, 20.00)	5366.352	10,382.921	1.935
50	114.02, 71.23	56.41	(58.74, 60.00) (138.85, 20.58)	2825.903	5458.501	1.932
70	104.72, 72.58	70.04	(35.81, 60.00) (150.99, 20.00)	5368.424	10,362.625	1.930
100	115.39, 84.07	70.74	(48.86, 60.00) (145.38, 20.00)	3449.49	6641.772	1.925
120	103.61, 69.47	58.00	(46.39, 60.00) (136.54, 21.72)	3730.166	7174.276	1.923
150	122.07, 87.60	72.47	(55.06, 60.00) (148.18, 20.00)	3013.208	5788.085	1.921
200	126.57, 100.49	70.38	(74.86, 52.74) (120.78, 30.35)	1316.13	2529.296	1.921

Table 11 Results for minimum FoS achieved by BBO over different iterations

No. of generation	Center point (a, b)	Radius (R)	Intersection points $(x_u, y_u), (x_l, y_l)$	Deriving moments (F_d)	Resisting moments (F_r)	FoS
10	101.49, 72.53	63.94	(38.79, 60.00) (138.80, 20.60)	4386.113	8501.784	1.938
20	108.31, 96.41	88.35	(27.82, 60.00) (152.66, 20.00)	10,024.444	5176.243	1.937
50	113.30, 98.34	79.31	(43.87, 60.00) (135.56, 22.22)	3061.430	5907.505	1.930
70	120.20, 104.11	85.55	(46.89, 60.00) (138.80, 20.60)	2926.120	5646.604	1.930
100	122.07, 108.42	94.17	(41.29, 60.00) (154.49, 20.00)	3795.981	7300.737	1.923
120	110.46, 105.21	92.59	(29.65, 60.00) (146.69, 20.00)	4507.961	8644.631	1.918
150	108.15, 90.35	73.22	(41.52, 60.00) (135.30, 22.35)	3408.054	6530.142	1.916
200	115.21, 114.35	77.80	(59.55, 60.00) (107.22, 36.96)	1364.78	2614.97	1.916

Table 12 Global minima safety factor computation using grid search

Slice no.	c (KPa)	μ (KPa)	ϕ (°)	b (m)	l (m)	h (m)	w (m)	α (°)	Resisting moment (F_r) $cl + (w\cos\alpha - \mu l)\tan\phi$	Deriving moment (F_d) $w\sin\alpha$
1	29	0	20	6.372	6.481	1.102	132.36	−9.131	235.623	−21.002
2	29	0	20	6.372	6.55	2.941	353.171	−13.392	315.362	−81.786
3	29	0	20	6.372	6.69	4.273	513.097	−17.7	372.438	−155.998
4	29	0	20	6.372	6.879	5.065	608.129	−22.140	404.846	−229.186
5	29	0	20	6.372	7.125	5.268	632.457	−26.531	414.484	−282.497
6	29	0	20	6.372	7.484	4.812	577.779	−31.511	396.727	−301.975
7	29	0	20	6.372	7.937	3.598	432.051	−36.602	356.582	−257.598
8	29	0	20	6.372	8.597	1.474	177.021	−42.022	297.114	−118.495
Factor of safety (FoS) $= \sum_{i=1}^{n} \frac{F_r}{F_d}$									FoS = 1.928	

Table 13 Global minima safety factor computation using genetic algorithm

Slice no.	c (KPa)	μ (KPa)	ϕ (°)	b (m)	l (m)	h (m)	w (m)	α (°)	Resisting moment (F_r) $cl + (w\cos\alpha - \mu l)\tan\phi$	Deriving moment (F_d) $w\sin\alpha$
1	29	0	20	5.739	5.783	1.103	119.321	−7.075	210.796	−14.689
2	29	0	20	5.739	5.864	2.949	318.872	−11.815	283.586	−65.259
3	29	0	20	5.739	5.99	4.294	464.343	−16.639	335.56	−132.897
4	29	0	20	5.739	6.172	5.106	552.128	−21.588	365.761	−203.047
5	29	0	20	5.739	6.424	5.334	576.758	−26.713	373.747	−259.139
6	29	0	20	5.739	6.773	4.902	530.067	−32.079	359.814	−281.388
7	29	0	20	5.739	7.26	3.696	399.644	−37.783	325.473	−244.743
8	29	0	20	5.739	7.971	1.532	165.664	−43.966	274.559	−114.963
Factor of safety (FoS) $= \sum_{i=1}^{n} \frac{F_r}{F_d}$									FoS = 1.921	

Table 14 Global minima safety factor computation using BBO algorithm

Slice no.	c (kPa)	μ (kPa)	ϕ (°)	b (m)	l (m)	h (m)	w (m)	α (°)	Resisting moment (F_r) $cl + (w\cos\alpha - \mu l)\tan\phi$	Deriving moment (F_d) $w\sin\alpha$
1	29	0	20	5.959	6.019	1.087	122.081	−8.112	218.561	−17.201
2	29	0	20	5.959	6.115	2.907	326.368	−12.547	293.12	−70.861
3	29	0	20	5.959	6.235	4.235	475.44	−17.120	346.014	−139.957
4	29	0	20	5.959	6.426	5.039	565.679	−21.777	377.373	−209.616
5	29	0	20	5.959	6.663	5.271	591.75	−26.581	386.023	−264.684
6	29	0	20	5.959	6.994	4.862	545.889	−31.618	371.884	−286.119
7	29	0	20	5.959	7.463	3.711	416.604	−36.923	337.54	−250.253
8	29	0	20	5.959	8.098	1.658	186.174	−42.634	284.455	−126.088
Factor of safety (FoS) $= \sum_{i=1}^{n} \frac{F_r}{F_d}$									FoS = 1.916	

Table 17. From this table, it is seen that for a given slip surface associated with optimum FoS value obtained in case study 1, the maximum error (%) is nearly 9.8% which is a minimum error as compared to computed value 10.11 and 11.05% by grid search and GA, whereas in case 2, the maximum error (%) for the optimum factor of safety value by BBO method is nearly 2.45%, which is also found least as compared to 4.3 and 4.9% by grid search and GA. In addition to this, the present approach has been easily implemented without additional computational complexity. It utilizes better solution quality with stable convergence rate and local minima avoidance. The algorithm provides a

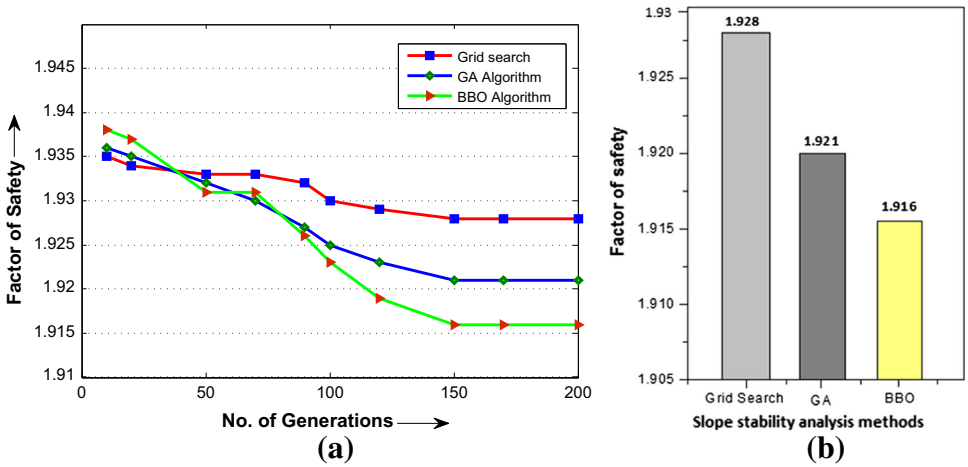

Fig. 11 The variation of FoS with no. of generation over presented methods. **a** Factor of safety versus generation graph and **b** factor of safety versus different methods

Table 15 Tuned parameters of BBO algorithm in case study 2

Number of habitats	100
Emigration rate (E)	1
Immigration rate (I)	1
M_{max}	0.2
Number of generation	200

viable tool that allows users to gain information about safety factor in a large search space. Based on these advantages the BBO algorithm acquired the highest stability analysis.

Table 16 Comparative summary of factor of safety's results for case study 2

Optimization algorithms	LEMs method	Minimum FoS
Fredlund and Krahn [31]	Fellenius method	1.928
Fredlund and Krahn [31]	Simplified Bishop method	2.080
Fredlund and Krahn [31]	Spencer	2.073
Fredlund and Krahn [31]	Janbu simplified method	2.041
Fredlund and Krahn [31]	Janbu rigorous method	2.008
Fredlund and Krahn [31]	M-P method	2.076
SSDP (Baker [54])	Spencer	1.98
Grid search (current study)	Fellenius method	1.928
GA (current study)	Fellenius method	1.921
BBO method (current study)	Fellenius method	1.916

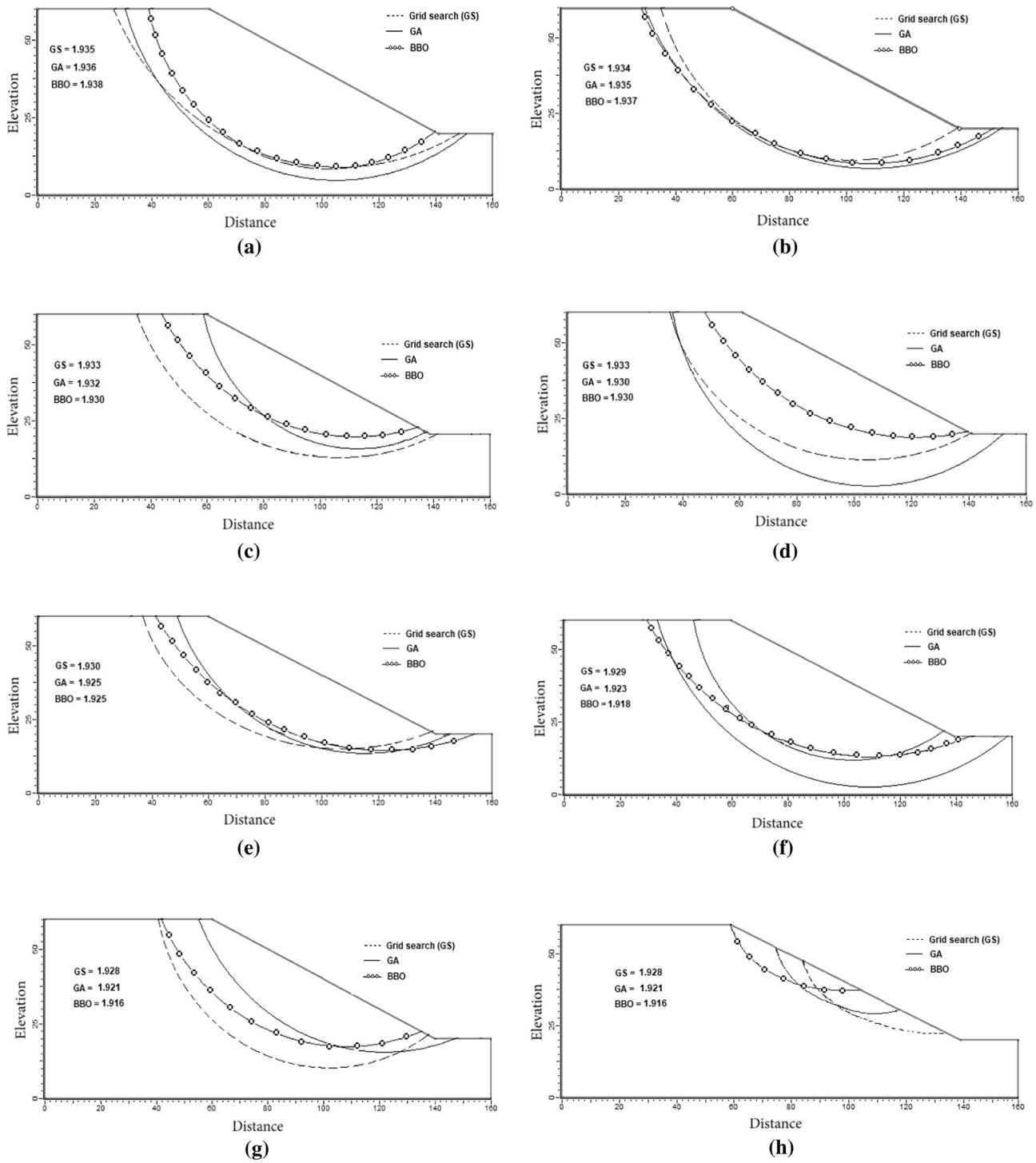

Fig. 12 Critical failure surfaces determined with Fellenius method over different generations. **a** Minimum FoS at generation 10, **b** minimum FoS at generation 20, **c** minimum FoS at generation 50, **d** minimum FoS at generation 70, **e** minimum FoS at generation 100, **f** minimum FoS at generation 120, **g** minimum FoS at generation 150 and **h** minimum FoS at generation 200

Table 17 The maximum error (%) analysis between the presented methods and slide tool evaluation

Case study	No. of generation	Grid search	GA	BBO	Rocscience slide tool			Error (in %)		
					Grid search	GA	BBO	Grid search	GA	BBO
Case study 1	10	1.335	1.341	1.344	1.463	1.411	1.413	9.588	5.219	5.133
	20	1.329	1.33	1.336	1.581	1.548	1.422	18.961	16.390	6.437
	50	1.324	1.322	1.328	1.57	1.506	1.434	18.580	13.918	7.981
	70	1.317	1.300	1.309	1.421	1.424	1.376	7.896	9.538	5.118
	100	1.302	1.29	1.296	1.395	1.393	1.4	7.142	7.984	8.024
	150	1.278	1.254	1.248	1.414	1.393	1.354	10.641	11.084	8.493
	200	1.265	1.237	1.224	1.464	1.368	1.345	15.731	10.590	9.885
	250	1.265	1.237	1.224	1.392	1.373	1.344	10.110	11.059	9.803
Case study 2	10	1.935	1.936	1.938	2.02	2.038	2.073	4.392	5.268	6.965
	20	1.934	1.935	1.937	2.03	2.000	1.997	4.963	3.359	3.097
	50	1.933	1.932	1.93	2.045	2.079	1.985	5.794	7.608	2.849
	70	1.933	1.93	1.93	2.026	2.08	1.973	4.811	7.772	2.227
	100	1.93	1.925	1.923	2.008	2.045	1.974	4.041	6.233	2.652
	120	1.929	1.923	1.918	2.041	2.075	1.973	5.806	7.904	2.867
	150	1.928	1.921	1.916	2.064	2.02	1.983	7.053	5.153	3.496
	200	1.928	1.921	1.916	2.023	2.005	1.963	4.927	4.372	2.453

7 Conclusion and future work

The BBO algorithm provides a viable tool to solve complex and nonlinear-type geotechnical problems. The proposed analysis allows the user to gain information about stability evaluation in a large solution space. From the detail discussion of this paper, it is found that the BBO algorithm is a suitable technique for employing to locate critical failure surface. Based on the findings, it appears that the stability analysis procedure makes BBO approach more efficient and applicable to achieve the reasonable factor of safety. In addition, the procedure followed for stability analysis eliminates invalid slip surfaces, which yields an unreasonable factor of safety. Hence the valid surfaces under the geometric and kinematic constraints were evaluated. The validation and performance of the algorithm were investigated by solving two different numerical benchmark case studies adopted from the literature. The findings of the study indicate that the BBO algorithm presents more consistent results with least percentage error as compared to previously developed methods such as grid search and GA. Nevertheless, the modifications to the proposed algorithm are still needed to continuously enhance the performance. Nonhomogeneous soil and rock slope models with water and load conditions in their stability analysis may be tried to explore more in future.

Compliance with ethical standards

Conflict of interest We hereby declare that we are having no conflict of interest

References

1. Vageesha S, Mathada G, Venkatachalam G, Srividya A (2007) Slope stability assessment-a comparison of probabilistic, possibilistic and hybrid approaches. Int J Perform Eng 3(2):231–242
2. Dodagoudar GR, Venkatachalam G (2000) Reliability analysis of slopes using fuzzy sets theory. Comput Geotech 27(2):101–115
3. Rubio E, Hall JW (2004) Uncertainty analysis in a slope hydrology and stability model using probabilistic and imprecise information. Comput Geotech 31(7):529–536
4. Zhang Z, Liu Z, Zheng L, Zhang Y (2014) Development of an adaptive relevance vector machine approach for slope stability inference. Neural Comput Appl 25(7–8):2025–2035
5. Aryal KP (2006) Slope stability evaluations by limit equilibrium and finite element methods. Ph.D. thesis, Norwegian University of Science and Technology
6. Fellenius W (1936) Calculation of the stability of earth dams. In: Transactions of the 2nd congress on large dams, Washington, DC, vol 4, pp 445–463. International Commission on Large Dams (ICOLD), Paris
7. Bishop AW (1955) The use of the slip circle in the stability analysis of slopes. Geotechnique 5(1):7–17
8. Morgenstern NR, Eo V, Eo Price V (1965) The analysis of the stability of general slip surfaces. Geotechnique 15(1):79–93
9. Spencer E (1967) A method of analysis of the stability of embankments assuming parallel inter-slice forces. Geotechnique 17(1):11–26

10. Janbu N (1975) Slope stability computations: In: Hirschfeld RC, Poulos SJ (eds) Embankment-dam engineering. Wiley, New York, 1973. Int J Rock Mech Min Sci Geomech Abstr 12: 67 (Pergamon)
11. Abramson LW (2002) Slope stability and stabilization methods. Wiley, New York
12. Ching RKH, Fredlund DG (1983) Some difficulties associated with the limit equilibrium method of slices. Canad Geotech J 20(4):661–672
13. Baker R, Garber M (1978) Theoretical analysis of the stability of slopes. Geotechnique 28(4):395–411
14. Greco VR (1996) Efficient monte carlo technique for locating critical slip surface. J Geotech Eng 122(7):517–525
15. Yamagami T, Ueta Y (1986) Noncircular slip surface analysis of the stability of slopes. Landslides 22(4):8–16
16. Kaswan A, Singh V, Jana PK (2018) A novel multi-objective particle swarm optimization based energy efficient path design for mobile sink in wireless sensor networks. Pervasive Mobile Comput. https://doi.org/10.1016/j.pmcj.2018.02.003
17. Kaswan A, Tomar A, Jana PK (2018) A GSA-based scheduling scheme for mobile charger in on-demand wireless rechargeable sensor networks. J Network Comp Appl. https://doi.org/10.1016/j.jnca.2018.02.017
18. Singh J, Verma AK, Banka H et al (2016) A study of soft computing models for prediction of longitudinal wave velocity. Arab J Geosci 9:224
19. Das SK, Tripathi S (2017) Adaptive and intelligent energy efficient routing for transparent heterogeneous ad-hoc network by fusion of game theory and linear programming. Appl Intell. doi:10.1007/s10489-017-1061-6
20. Chen Z, Morgenstern NR (1983) Extensions to the generalized method of slices for stability analysis. Canad Geotech J 20(1):104–119
21. McCombie P, Wilkinson P (2002) The use of the simple genetic algorithm in finding the critical factor of safety in slope stability analysis. Comput Geotech 29(8):699–714
22. Sarat Kumar Das (2005) Slope stability analysis using genetic algorithm. Electron J Geotech Eng 10:429–439
23. Zolfaghari AR, Heath AC, McCombie PF (2005) Simple genetic algorithm search for critical non-circular failure surface in slope stability analysis. Comput Geotech 32(3):139–152
24. Sun J, Li J, Liu Q (2008) Search for critical slip surface in slope stability analysis by spline-based ga method. J Geotech Geoenviron Eng 134(2):252–256
25. Sengupta A, Upadhyay A (2009) Locating the critical failure surface in a slope stability analysis by genetic algorithm. Appl Soft Comp 9(1):387–392
26. Kahatadeniya KS, Nanakorn P, Neaupane KM (2009) Determination of the critical failure surface for slope stability analysis using ant colony optimization. Eng Geol 108(1):133–141
27. Ahangar-Asr A, Faramarzi A, Javadi AA (2010) A new approach for prediction of the stability of soil and rock slopes. Eng Comput 27(7):878–893
28. Khajehzadeh M, Taha MR, El-Shafie A, Mohammad K (2011) Search for critical failure surface in slope stability analysis by gravitational search algorithm. Int J Phys Sci 6(21):5012–5021
29. Khajehzadeh M, Taha MR, El-Shafie A, Eslami M (2012) A modified gravitational search algorithm for slope stability analysis. Eng Appl Artif Intell 25(8):1589–1597
30. Kashani AR, Gandomi AH, Mousavi M (2016) Imperialistic competitive algorithm: a metaheuristic algorithm for locating the critical slip surface in 2-dimensional soil slopes. Geosci Front 7(1):83–89
31. Fredlund DG, Krahn J (1977) Comparison of slope stability methods of analysis. Canad Geotech J 14(3):429–439
32. Cheng YM, Lau CK (2014) Slope stability analysis and stabilization: new methods and insight. CRC Press, Boca Raton
33. Huang YH (2014) Slope stability analysis by the limit equilibrium method: fundamentals and methods. American Society of Civil Engineers, Reston
34. Krahn J (2003) The 2001 rm hardy lecture: the limits of limit equilibrium analyses. Canad Geotech J 40(3):643–660
35. Wu A (2012) Locating general failure surfaces in slope analysis via cuckoo search. https://www.rocscience.com/help/slide/webhelp7/pdf_files/theory/. Accessed 27 Jan 2017
36. Cheng YM, Li L, Chi SC (2007) Performance studies on six heuristic global optimization methods in the location of critical slip surface. Comput Geotech 34(6):462–484
37. Chen Z-Y, Shao C-M (1988) Evaluation of minimum factor of safety in slope stability analysis. Canad Geotech J 25(4):735–748
38. Nguyen VU (1985) Determination of critical slope failure surfaces. J Geotech Eng 111(2):238–250
39. Cheng YM (2003) Location of critical failure surface and some further studies on slope stability analysis. Comput Geotech 30(3):255–267
40. Abdallah I, Husein Malkawi AI, Hassan WF, Sarma SK (2001) Global search method for locating general slip surface using monte carlo techniques. J Geotech Geoenviron Eng 127(8):688–698
41. Jade S, Shanker KD (1995) Modelling of slope failure using a global optimization technique. Eng Optim+ A35 23(4):255–266
42. Simon D (2008) Biogeography-based optimization. IEEE Trans Evol Comput 12(6):702–713
43. Yang G, Zhang Y, Yang J, Ji G, Dong Z, Wang S, Feng C, Wang Q (2016) Automated classification of brain images using wavelet-energy and biogeography-based optimization. Multimed Tools Appl 75(23):15601–15617
44. Wang S, Zhang Y, Ji G, Yang J, Jianguo W, Wei L (2015) Fruit classification by wavelet-entropy and feedforward neural network trained by fitness-scaled chaotic abc and biogeography-based optimization. Entropy 17(8):5711–5728
45. Yadav RK, Banka H (2016) Ibbomsa: an improved biogeography-based approach for multiple sequence alignment. Evol Bioinform 12:237
46. Song Y, Liu M, Wang Z (2010) Biogeography-based optimization for the traveling salesman problems. In: 2010 Third international joint conference on computational science and optimization (CSO), vol 1, pp 295–299. IEEE
47. MacArthur R, Wilson E (1967) The theory of biogeography. Princeton University Press, Princeton
48. Guo W, Chen M, Wang L, Mao Y, Wu Q (2017) A survey of biogeography-based optimization. Neural Comput Appl 28(8):1909–1926
49. Das SK, Tripathi S (2017) Energy efficient routing formation technique for hybrid ad hoc network using fusion of artificial intelligence techniques. Int J Commun Syst 30(16)1–16. https://doi.org/10.1002/dac.3340
50. Lalwani P, Banka H, Kumar C (2016) BERA: a biogeography-based energy saving routing architecture for wireless sensor networks. Soft Comput 22(5):1651–1667
51. Slide search methods (2016) https://www.rocscience.com/help/slide/webhelp7/pdf_files/developer_tips/Slide_Search_Methods.pdf/. Accessed 19 July 2017
52. Kostic S, Vasovic N, Sunaric D (2015) A new approach to grid search method in slope stability analysis using box-behnken statistical design. Appl Math Comput 256:425–437
53. Solati S, Habibagahi G (2006) A genetic approach for determining the generalized interslice forces and the critical non-circular slip surface. Iran J Sci Technol Trans B Eng 30(1):1–20
54. Baker R (1980) Determination of the critical slip surface in slope stability computations. Int J Numer Anal Methods Geomech 4(4):333–359
55. Rocscience slide. https://www.rocscience.com/rocscience/products/slide. Accessed 10 Dec 2016